

# A microcontact printing induced supramolecular self-assembled photoactive surface for patterning polymer brushes†

Cite this: *Chem. Commun.*, 2013, **49**, 11167

Received 7th August 2013,  
Accepted 8th October 2013

DOI: 10.1039/c3cc46037a

www.rsc.org/chemcomm

**A facile and robust strategy for creating micropatterned polymer brushes via the combination of a micro-contact printing ( $\mu$ CP) induced supramolecular self-assembled photoactive surface with subsequent self-initiated photografting and photopolymerization (SIPGP) is reported. The results contribute to polymeric functionalization on a wide range of hydroxylated surfaces or graphene based materials.**

Polymer brushes with a well controllable functionality, density and thickness at almost molecular precision for smart surfaces, which can interact with and respond well to environments, have attracted tremendous interest because of their potential applications in many surface-based technologies.<sup>1–3</sup> The patterned one, particularly useful for array-based platforms and for the study of stimuli-responsive phenomena, can be fabricated via the combination of the creation of a self-assembled monolayer (SAM) template by a variety of lithographic strategies and subsequent amplification via surface initiated polymerization (SIP).<sup>4</sup> Among these lithographic methods, microcontact printing ( $\mu$ CP) is a simple and cost-effective tool to pattern microscale initiator SAMs as templates on a solid substrate, such as silicon<sup>5</sup> or Au,<sup>6</sup> giving the correct choice of the anchor group and mesogen. In addition to the direct printing chemical functionality,  $\mu$ CP has also been used for chemical reaction under nanoscale confinement when the inked stamp is in contact with a functional substrate that is able to react chemically with the reactive ink molecules from a structured polydimethylsiloxane (PDMS) stamp.<sup>7</sup>

Most research studies were focused on fabricating polymer brushes with covalent modification of a substrate from a surface confined initiator and subsequent SIP. There are only few cases in which noncovalent strategies have been used to achieve initiator

attachment. Recently, Becer *et al.*<sup>8</sup> reported that a hydrogen bonded initiator attached to the HOOC-terminated substrate steadily, resulting in a suitable template for grafting polymer brushes. Zhou *et al.*<sup>9</sup> demonstrated atom transfer radical polymerization (ATRP) which involves transfer of a pyrene-terminated macroinitiator to a graphene oxide film via  $\pi$ - $\pi$  stacking interactions with further amplification of polymer brushes. The majority of research studies reporting fabrication of polymer brushes make use of the SIP via the amplification of the initiator SAM template. More recently, it was demonstrated that patterned polymer brushes can also be prepared even without a surface-bound initiator by self-initiated photografting and photopolymerization (SIPGP) on patterned SAMs,<sup>10</sup> on carbon deposits,<sup>5</sup> or by the direct use of a surface chemical contrast.<sup>11</sup> The SIPGP allows us to have a robust choice due to its several advantages including no additional surface analog reaction to introduce a photo-initiator for SIP and very stable covalent attachment of the polymer brush to the surface via C–C bonds.

Herein, we developed the  $\mu$ CP technology to induce supramolecular self-assembly forming a photoactive surface for fabricating micropatterned polymer brushes via subsequent amplification of SIPGP.  $\mu$ CP is thus used to direct the supramolecular assembly of Py-CH<sub>2</sub>NH<sub>2</sub> via a hydrogen bond onto an OH-terminated silicon substrate to form an active surface. This successful strategy is then moved to functionalize the graphene via  $\pi$ - $\pi$  interaction with Py-CH<sub>2</sub>NH<sub>2</sub> for further improving graphene's surface chemical properties and extending the applications. Since the amine is a popular and effective group for photopolymerization,<sup>12</sup> the resulting photoactive pattern allows the subsequent grafting of polymer brushes via the robust SIPGP.

Our strategies of  $\mu$ CP inducing a supramolecular self-assembled photoactive surface for patterning polymer brushes are schematically shown in Fig. 1. A Py-CH<sub>2</sub>NH<sub>2</sub> solution inked PDMS stamp was first made to come into contact with the OH-terminated silicon substrate, which was treated with fresh piranha solution (Fig. 1A and B) with gentle force, followed by rinsing with ethanol and drying in N<sub>2</sub> flow. The NH<sub>2</sub>-terminated pyrene derivatives interact with the HO-terminated surface by a hydrogen bond and the pyrene groups with each other through  $\pi$ - $\pi$  stacking interactions

<sup>a</sup> Division of Polymer and Composite Materials, Ningbo Institute of Material Technology and Engineering, Chinese Academy of Science, Ningbo 315201, China. E-mail: tao.chen@nimte.ac.cn

<sup>b</sup> State Key Laboratory of Polymer Physics and Chemistry, Changchun Institute of Applied Chemistry, Chinese Academy of Sciences, Changchun 130022, China

<sup>c</sup> Faculty of Materials Science and Chemical Engineering, Ningbo University, Ningbo 315211, China

† Electronic supplementary information (ESI) available. See DOI: 10.1039/c3cc46037a

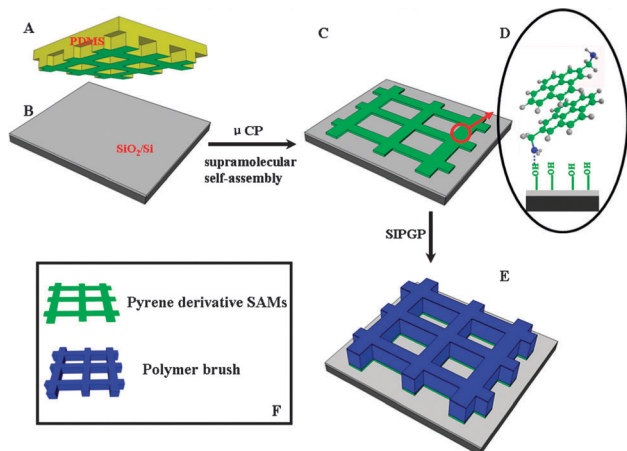


**Fig. 1** Schematic procedure for fabricating patterned polymer brushes on silicon-based substrates via  $\mu$ CP directed supramolecular self-assembly and SIPGP.

simultaneously with the amino group pointing toward the outer interface (Fig. 1C and D). Such a structure offered activity sites for grafting polymer brushes by final SIPGP of styrene or other vinyl monomers (Fig. 1E).

To test preliminarily whether there was a successful attachment of  $\text{Py-CH}_2\text{NH}_2$  to the hydroxylated silicon surface by the  $\mu$ CP induced supramolecular self-assembly, water contact angle (CA) measurement was done to investigate the surface properties of silicon before and after  $\text{Py-CH}_2\text{NH}_2$  modification. Fig. 2A shows that the CA of the silicon substrate, treated with a fresh piranha solution, is  $14^\circ$ . After patterned modification with  $\text{Py-CH}_2\text{NH}_2$ , the value increased to  $55^\circ$ , indicating that the functional surface became less hydrophilic (Fig. 2B). In order to indirectly evidence our supramolecular self-assembly mechanism, the flat stamp was employed to generate a homogenous active surface on a silicon substrate. As shown in Fig. S1A provided in the ESI,<sup>†</sup> the value of the contact angle of the silicon surface modified by an unpatterned pyrene derivative is  $67^\circ$ , which shows that the hydroxyl-terminated silicon surface is covered fully with amine-groups. After subsequent amplification modification by a polystyrene (PS) brush, the patterned and unpatterned surfaces have a water CA of  $96^\circ$  and  $102^\circ$ , respectively, indicating significant hydrophobic properties of PS (Fig. 2C and Fig. S1B, ESI<sup>†</sup>). The difference in hydrophilic/hydrophobic properties of the patterned active surface and the subsequent grafted polymer brush suggested a supramolecular structure.

The X-ray photoelectron spectrum (XPS) and attenuated total reflectance Fourier transform infrared spectroscopy (ATR-FTIR) were further used to investigate the supramolecular interaction and subsequent polymer brush amplification. In order to achieve a high quality XPS spectrum, an unpatterned  $\text{Py-CH}_2\text{NH}_2$  supramolecular active surface was used, which is shown in Fig. 3A and Fig. S2 (ESI<sup>†</sup>). The N 1s spectrum shows peaks attributable to hydrogen bonded  $\text{NH}_2$



**Fig. 2** Static water contact angle measurements for (A) silicon wafer treated by fresh piranha solution. (B) Patterned  $\text{Py-CH}_2\text{NH}_2$  active surface on the silicon substrate. (C) Polystyrene brushes grafted from the patterned  $\text{Py-CH}_2\text{NH}_2$  coated silicon substrate.

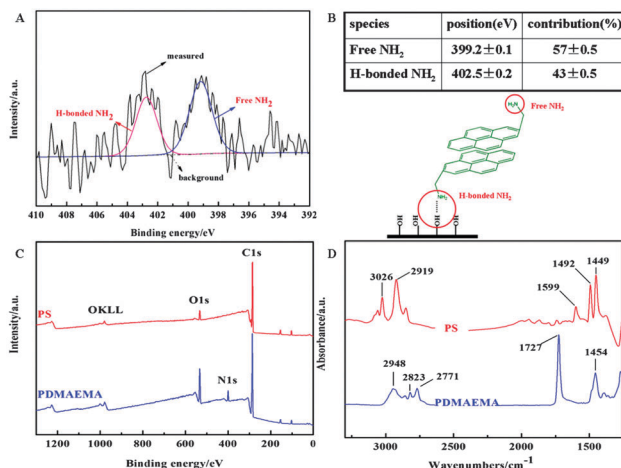


**Fig. 3** (A) High resolution XPS spectra of homogenous  $\text{Py-CH}_2\text{NH}_2$  modified silicon of N 1s. (B) Quantification of the N 1s XPS spectrum of A and possible supramolecular self-assembly mechanism. (C) XPS survey scans and (D) ATR-IR spectra of PS and PDMAEMA brushes on silicon surfaces.

at about 402.5 eV and free  $\text{NH}_2$  terminal groups at  $\sim 399.0$  eV. The two different N atoms are attributed to the hydrogen bond between  $\text{Si-OH}$  and  $\text{NH}_2$  and the free  $\text{NH}_2$  towards the outer interface of the active surface.<sup>13</sup> Fig. 3B shows quantification of the high resolution spectra shown in Fig. 3A. The ratio of the hydrogen bond N 1s peak to the free N 1s peak is approximately 43/57. The results significantly evidenced the supramolecular self-assembly mechanism and structure. XPS analyses of PS and poly(*N,N*-dimethylaminoethyl methacrylate) (PDMAEMA) brushes are shown in Fig. 3C. For the PS brush, only C 1s and O 1s peaks are visible, at 285.0 and 533.0 eV, respectively. The small O 1s peak is attributed to water adsorption.<sup>11</sup> The N 1s peak present in the PDMAEMA spectrum is centered at 405.0 eV. The results reveal the successful polymerization of monomers and feasibility of the  $\mu$ CP induced supramolecular self-assembly strategy. The ATR-FTIR spectrum in Fig. 3D displays the successful grafting PS and PDMAEMA brushes. Additionally, block copolymers can be easily formed, given the presence of possible attractable hydrogen atoms.

After amplifying the photoactive surface with SIPGP of a monomer, atomic force microscopy (AFM) was employed to ascertain the  $\mu$ CP directed supramolecular self-assembled active surface and amplified polymer brushes. Fig. 4A shows an AFM image of the active surface patterned with a feature size of  $\sim 10 \mu\text{m}$  and the layer thickness of approximately 2.0 nm. This value is in good agreement with the theoretical height of two layer active surfaces formed by  $\pi$ - $\pi$  stacking interactions, resulting in potential  $\text{NH}_2$ -terminated groups on the top layer. The AFM images of the resulting patterned polymer brushes are shown in Fig. 4B and Fig. S3A (ESI<sup>†</sup>). The corresponding 3D images of patterned/homogenous polymer brushes are also displayed in Fig. S4 (ESI<sup>†</sup>). It can be seen that the pattern size of the polymer brush grid is  $\sim 10 \mu\text{m}$ , indicating a well-controlled selectivity polymerization on functionalized sites. The result indicates that the amino-functionalized surface shows high activity in comparison with the hydroxyl-functionalized silicon surface.<sup>10-12</sup>

Based on  $\pi$ - $\pi$  stacking interaction,<sup>9</sup> our strategy of  $\mu$ CP directed supramolecular self-assembly can also be employed to graphene-based materials including a GO (graphene oxide) film,

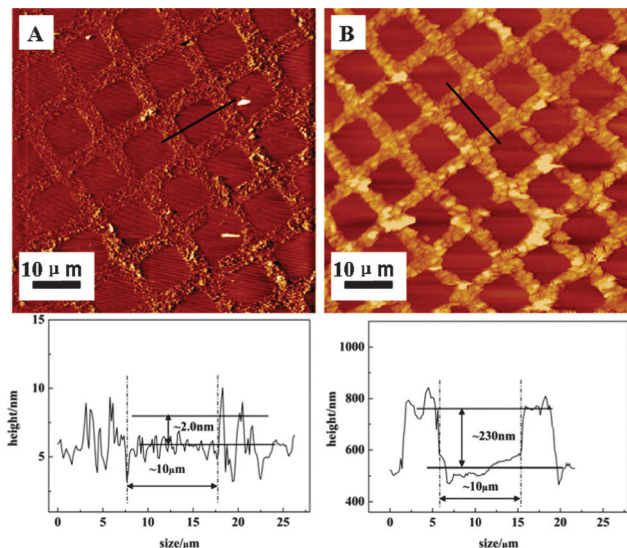


**Fig. 4** Tapping-mode AFM height images ( $80 \mu\text{m} \times 80 \mu\text{m}$ ) and the selected corresponding height profile of (A) patterned  $\text{Py-CH}_2\text{NH}_2$  on a hydroxylated silicon surface and (B) patterned PS brushes grafted from the silicon surface by SIPGP.

RGO (reduced graphene oxide), epitaxial graphene on SiC and CVD (chemical vapor deposition) graphene, followed by SIPGP to further achieve a specific polymer chemical functionality on graphene-based materials and extend their applications.<sup>14</sup> Fig. 5A displays the AFM height image of single layer CVD graphene transferred on a silicon substrate with visible wrinkles on the film. As displayed in Fig. 5B, the thickness of the patterned  $\text{Py-CH}_2\text{NH}_2$  active surface on graphene is about 3.6 nm, showing a several layer stack of  $\text{Py-CH}_2\text{NH}_2$ . After amplification of the active surface by SIPGP, PS brushes about 200 nm in size were grafted from the patterned active area from graphene (Fig. 5C). The unpatterned areas on graphene display the homogenous PS brush with a thin thickness grafted from existing defect sites of graphene, which corresponds well with previous work (Fig. S4A, ESI<sup>†</sup>),<sup>15</sup> showing the high activity of the  $\text{NH}_2$ -terminated active surface compared with graphene. Fig. 5D shows the Raman spectrum of pristine graphene (a),  $\text{Py-CH}_2\text{NH}_2$  patterned graphene (b) and PS brushes on graphene (c). The CVD graphene shows the significant single

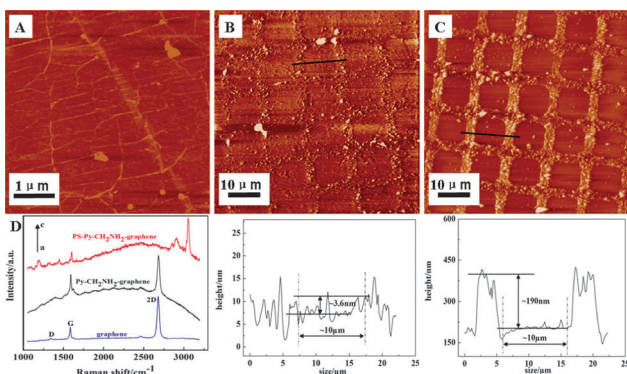


**Fig. 5** AFM height images and selected corresponding height profile of (A) pristine single layer graphene on the silicon substrate ( $5 \mu\text{m} \times 5 \mu\text{m}$ ). (B) Patterned  $\text{Py-CH}_2\text{NH}_2$  and (C) PS brush grafted from the active surface on graphene ( $80 \mu\text{m} \times 80 \mu\text{m}$ ). (D) Raman spectrum of (a) single layer CVD graphene, (b)  $\text{Py-CH}_2\text{NH}_2$  patterned graphene and (c) PS brush grafted from patterned graphene.

layer graphene spectrum of the D, G and 2D mode. However, after patterning with  $\text{Py-CH}_2\text{NH}_2$ , it was not possible to obtain a high quality Raman spectrum due to the large luminescence effect of  $\text{Py-CH}_2\text{NH}_2$ . The Raman spectrum of PS brushes on graphene contains the PS scattering intensity in the range of  $\nu = 1200\text{--}1600 \text{ (cm}^{-1}\text{)}$  and  $\nu = 3000\text{--}3100 \text{ (cm}^{-1}\text{)}$ . Whereas there is apparent spectral overlap in the region of the D and G bands between PS and graphene. Due to the luminescence background with a broad peak between 1700 and 2700  $\text{(cm}^{-1}\text{)}$  from the patterned  $\text{Py-CH}_2\text{NH}_2$  on the graphene surface and the highly increased layer thickness of polymer film, the 2D mode of graphene is difficult to be observed.

We have presented a simple and robust strategy to fabricate micropatterned polymer brushes from a hydroxylated silicon surface and graphene *via* a  $\mu\text{CP}$  induced supramolecular self-assembled photoactive surface, followed by SIPGP. A more cheap and commercial glass substrate, covered with massive hydroxyl groups after treatment with piranha solution, was also employed as the targeted substrate for coating polymer brushes by the combination of  $\mu\text{CP}$  induced supramolecular self-assembly and SIPGP. Our patterning strategy can most likely be extended to a wide range of monomers and various universal substrates (hydroxylated and graphene-based substrate surfaces) that can form supramolecular self-assembly with active moieties, and thus provide a simple, robust and powerful method to create a polymeric chemically functionalized surface.

We thank the Chinese Academy of Science for Hundred Talents Program, the Chinese Central Government for Thousand Young Talents Program, and the Open Research Fund of State Key Laboratory of Polymer Physics and Chemistry, Changchun Institute of Applied Chemistry, Chinese Academy of Sciences.

## Notes and references

- 1 S. Edmondson, V. L. Osborne and W. T. S. Huck, *Chem. Soc. Rev.*, 2004, **33**, 14–22.
- 2 I. Luzinov, S. Minko and V. V. Tsukruk, *Prog. Polym. Sci.*, 2004, **29**, 635–698.
- 3 M. A. C. Stuart, W. T. S. Huck, J. Genzer, M. Mueller, C. Ober, M. Stamm, G. B. Sukhorukov, I. Szleifer, V. V. Tsukruk, M. Urban, F. Winnik, S. Zauscher, I. Luzinov and S. Minko, *Nat. Mater.*, 2010, **9**, 101–113.
- 4 T. Chen, I. Amin and R. Jordan, *Chem. Soc. Rev.*, 2012, **41**, 3280–3296.
- 5 M. Steenackers, R. Jordan, A. Kuller and M. Grunze, *Adv. Mater.*, 2009, **21**, 2921–2925.
- 6 I. Amin, M. Steenackers, N. Zhang, R. Schubel, A. Beyer, A. Golzhauser and R. Jordan, *Small*, 2011, **7**, 683–687.
- 7 D. I. Rozkiewicz, D. Janczewski, W. Verboom, B. J. Ravoo and D. N. Reinhoudt, *Angew. Chem., Int. Ed.*, 2006, **45**, 5292–5296.
- 8 C. R. Becer, C. Haensch, S. Hoepfner and U. S. Schubert, *Small*, 2007, **3**, 220–225.
- 9 T. T. Gao, X. L. Wang, B. Yu, Q. B. Wei, Y. Q. Xia and F. Zhou, *Langmuir*, 2013, **29**, 1054–1060.
- 10 M. Steenackers, A. Kuller, S. Stoycheva, M. Grunze and R. Jordan, *Langmuir*, 2009, **25**, 2225–2231.
- 11 M. Steenackers, S. Q. Lud, M. Niedermeier, P. Bruno, D. M. Gruen, P. Feulner, M. Stutzmann, J. A. Garrido and R. Jordan, *J. Am. Chem. Soc.*, 2007, **129**, 15655–15661.
- 12 I. Amin, M. Steenackers, N. Zhang, A. Beyer, X. H. Zhang, T. Pirzer, T. Hugel, R. Jordan and A. Golzhauser, *Small*, 2010, **6**, 1623–1630.
- 13 R. G. Acres, A. V. Ellis, J. Alvino, C. E. Lenahan, D. A. Khodakov, G. F. Metha and G. G. Andersson, *J. Phys. Chem. C*, 2012, **116**, 6289–6297.
- 14 K. S. Novoselov, A. K. Geim, S. V. Morozov, D. Jiang, Y. Zhang, S. V. Dubonos, I. V. Grigorieva and A. A. Firsov, *Science*, 2004, **306**, 666–669.
- 15 M. Steenackers, A. M. Gigler, N. Zhang, F. Deubel, M. Seifert, L. H. Hess, C. Lim, K. P. Loh, J. A. Garrido, R. Jordan, M. Stutzmann and I. D. Sharp, *J. Am. Chem. Soc.*, 2011, **133**, 10490–10498.